Digital Signal Processing 69 (2017) 193–203

Contents lists available at ScienceDirect

Digital Signal Processing

www.elsevier.com/locate/dsp

A sparse direction-of-arrival estimation algorithm for MIMO radar in the presence of gain-phase errors

Jing Liu [a,b], Weidong Zhou [a,*], Xianpeng Wang [c], Defeng (David) Huang [b]

[a] College of Automation, Harbin Engineering University, Harbin 150001, China
[b] School of Electrical, Electronic and Computer Engineering, The University of Western Australia, Australia
[c] College of Information Science and Technology, Hainan University, Hainan, 570228, China

ARTICLE INFO

Article history:
Available online 10 July 2017

Keywords:
Multiple-input multiple-output radar
Direction-of-arrival estimation
Gain-phase errors
Fourth-order cumulants
Sparse representation

ABSTRACT

In this paper, the problem of direction-of-arrival (DOA) estimation for monostatic multiple-input multiple-output (MIMO) radar with gain-phase errors is addressed, by using a sparse DOA estimation algorithm with fourth-order cumulants (FOC) based error matrix estimation. Useful cumulants are designed and extracted to estimate the gain and the phase errors in the transmit array and the receive array, thus a reliable error matrix is obtained. Then the proposed algorithm reduces the gain-phase error matrix to a low dimensional one. Finally, with the updated gain-phase error matrix, the FOC-based reweighted sparse representation framework is introduced to achieve accurate DOA estimation. Thanks to the fourth-order cumulants based gain-phase error matrix estimation, and the reweighted sparse representation framework, the proposed algorithm performs well for both white and colored Gaussian noises, and provides higher angular resolution and better angle estimation performance than reduced-dimension MUSIC (RD-MUSIC), adaptive sparse representation (adaptive-SR) and ESPRIT-based algorithms. Simulation results verify the effectiveness and advantages of the proposed method.

1. Introduction

Compared with conventional phased-array radar, multiple-input multiple-output (MIMO) radar can achieve higher resolution and better parameter identification, thus it has drawn increasing interest [1]. According to the antenna configuration, MIMO radar can be classified into statistical MIMO radar with the spatial diversity [2], and colocated MIMO radar with the waveform diversity [3]. Based on the positions of the arrays, MIMO radar can be grouped into bistatic MIMO radar with transmit and receive arrays separated away from each other, and monostatic one with the arrays located closely. Therefore, in bistatic MIMO radar, direction-of-departure (DOD) and direction-of-arrival (DOA) are different, and they are equal in monostatic MIMO radar. In this paper, we will investigate the angle estimation problem in colocated MIMO radar equipped with closely-located arrays.

Angle estimation is an important problem in array signal processing, communication systems and radar applications [4,5]. A lot of algorithms have been proposed for DOA estimation, e.g. those based on subspace and sparse representation (SR). Conventional subspace-based methods such as MUSIC (multiple signal classification) [6], ESPRIT (estimation of signal parameters via rotational invariance techniques) [7] and Capon [8], have been extended to reduced-dimension Capon (RD-Capon) [9], Unitary ESPRIT [10] and so forth to estimate the DOA, which possess improved performance and low computation burden. It has been shown that the emerging sparse representation-based algorithms have remarkable advantages over alternative methods [11]. For example, they adapt better to the challenging circumstance of only a small number of snapshots available and achieve high angle resolution. A few SR-based algorithms have been proposed, such as l_1-SVD (singular value decomposition) [11], l_1-SRACV (sparse representation array covariance vectors) [12] and weighted-l_1-SRACV [13]. In [14], a covariance vector-based sparse representation algorithm was proposed to achieve the DOA estimation. With increased degrees of freedom, it extended the array aperture. In [15], exploiting the coefficients of the RD-Capon spatial spectrum, a reweighted l_1-norm penalty sparse representation method was proposed to obtain the DOA. Subspace-based methods rely heavily on the accuracy of array

* Corresponding author.
E-mail addresses: liujing@hrbeu.edu.cn (J. Liu), zhouweidong@hrbeu.edu.cn (W. Zhou), wangxianpeng@hrbeu.edu.cn (X. Wang), david.huang@uwa.edu.au (D. Huang).

http://dx.doi.org/10.1016/j.dsp.2017.06.025

manifold, which is also important for SR-based algorithms, because the array manifold has an impact on the construction of complete dictionary in SR-based methods and then the signal recovery [16]. However, in practical applications, two circumstances will degrade the DOA estimation performance: (I) The array manifold is often affected by gain-phase errors if the array is not calibrated well [17]; (II) The additive noises between antennas are often correlated, rather than white noises that exist in perfectly ideal condition [18]. Some algorithms [19–25] have been proposed to solve the two problems, which will be discussed in the following.

The performance of the methods mentioned above can be seriously degraded by gain-phase errors [17]. For subspace-based methods, to deal with the errors, a modified iterative MUSIC-like scheme [19] was proposed to estimate the DOAs by a large quantity of high complexity multiple peak searches. An ESPRIT-like method [20] was proposed to simultaneously obtain the angles and the errors with low complexity. Unlike [20], in [21] an ESPRIT-based algorithm was proposed by estimating the angles firstly, therefore it does not depend on the error matrix estimation and achieves better performance. Besides, with gain-phase errors, a RD-MUSIC algorithm [22] was proposed by one-dimensional peak searches, which achieves accurate DOA estimation. There are few works to cope with the gain-phase errors in SR-based algorithms. An adaptive sparse representation (adaptive-SR) algorithm [16] improves DOA estimation performance, by calibrating the dictionary dynamically and estimating the sparse solution adaptively. Unfortunately, adaptive-SR requires reasonable initial angles, and it is necessary for the errors to be small enough to keep the initial angles reliable. Consequently, although adaptive-SR algorithm performs well with small gain-phase errors, it is invalid and unable to be convergent with large gain-phase errors as will be shown in this paper.

When DOA estimation experiences spatially Gaussian colored noises, the above mentioned algorithms perform poorly, especially in low signal-to-noise ratio (SNR) region. Based on fourth-order cumulants (FOC), some algorithms like FOC-MUSIC [23] and FOC-ESPRIT [24] have been proposed to deal with colored noises. In [25], l_1-SRFOC algorithm achieves high resolution by solving a FOC-based sparse recovery problem. Unfortunately, for uniform linear arrays (ULAs) with array errors such as mutual coupling and gain-phase errors, FOC-based methods encounter serious performance degradation. Aiming at DOA estimation in MIMO radar in the presence of mutual coupling, in [26], a sparse representation approach based on FOC was proposed to suppress colored noises. However, the algorithm in [26] is invalid for the problem of DOA estimation with gain-phase errors.

The focus of this paper is to accurately estimate the DOAs for both white and colored Gaussian noises, by eliminating the effect of gain-phase errors. Although the subspace-based methods in [21] and [22] perform well in the presence of gain-phase errors via the eigendecomposition of covariance matrix of the received data, their performance degrades with colored noises. To deal with colored noises, conventional fourth-order cumulants-based methods can obtain the DOAs by constructing an FOC matrix [23,26]. However, as gain-phase errors are entirely unknown, subspace-based or SR-based methods cannot be applied directly to estimate DOAs. In this paper, for monostatic MIMO radar with gain-phase errors, an FOC-based sparse DOA estimation algorithm is proposed. Firstly, exploiting the well-calibrated parts of the arrays, useful cumulants are designed and extracted to estimate gain and phase errors in transmit and receive arrays, thus a reliable error matrix is obtained. Secondly, based on the dimensional reduction, a new gain-phase error matrix with a low dimension is obtained. Finally, with the error matrix, inspired by [26], the FOC-based reweighted sparse representation framework is introduced to obtain the DOAs. Simulation results show that the proposed method provides precise DOA estimation for both white and colored Gaussian noises, and with higher spatial angular resolution and better angle estimation performance, it outperforms RD-MUSIC, adaptive-SR and ESPRIT-based algorithms. Furthermore, unlike adaptive-SR algorithm [16], the performance of the proposed method is independent of gain and phase errors, and it behaves well no matter how large the errors are. Meanwhile, the performance of the proposed method does not depend on the correlation level of colored noise.

Compared with the DOA estimation method in [26], which deals with unknown mutual coupling, the proposed method deals with other array errors, i.e. gain-phase errors. In addition, the two methods have the following differences: (I) The error matrix structures and system models are different. Mutual coupling is modeled as a banded symmetric Toeplitz matrix in [26], while gain-phase errors are modeled as a diagonal matrix in this paper. As a result, they have different effects on the steering matrices. (II) The approaches of the error elimination are different. [26] uses a linear transformation, which causes the loss of array aperture and makes the error matrix direction-dependent. However, in this paper, new FOC-based gain and phase error estimation matrices are proposed without causing the aperture loss, and the estimated error matrix is direction-independent. Moreover, when eliminating the array errors, [26] does not apply the FOC, while in this paper the fourth-order cumulants are used to estimate the errors. (III) The dimensional reduction makes no difference on the matrix that contains the mutual coupling [26], whereas it transforms the estimated gain-phase error matrix into a new one in this paper.

Notation: $(\cdot)^{\mathrm{H}}$, $(\cdot)^{\mathrm{T}}$, $(\cdot)^{-1}$ and $(\cdot)^{*}$ denote conjugate-transpose, transpose, inverse and conjugate, respectively. $\otimes$ and $\odot$ denote Kronecker and Khatri–Rao product operators, respectively. $\mathbf{I}_K$ denotes a $K \times K$ dimensional unit matrix. $||\cdot||_1$, $||\cdot||_2$ and $||\cdot||_F$ denote the l_1 norm, the l_2 norm and the Frobenius norm, respectively. $\mathrm{diag}(\cdot)$ and $\mathrm{vec}(\cdot)$ denote the diagonalization operation and the vectorization operation, respectively.

2. System model

Consider a narrowband monostatic MIMO radar system. The numbers of the antennas in transmit array and receive array are M and N, respectively. Both arrays are half-wavelength spaced ULAs. As the transmit array and the receive array are closely located, the DOD and the DOA are assumed to be the same. The M transmitting antennas are used to transmit M orthogonal waveforms. At the receive array, the antennas are impinged by the echo signals from P uncorrelated targets located in the far-field, whose DOAs are denoted by θ_p, $p = 1, 2, \ldots, P$, respectively. When gain-phase errors are taken into account at both transmit array and receive array, at the receiver, the received signal reflected by the P targets is given by [27–32]

$$\mathbf{x}(l,t) = \sum_{p=1}^{P} \alpha_p(t)\tilde{\mathbf{a}}_r(\theta_p)\tilde{\mathbf{a}}_t^{\mathrm{T}}(\theta_p)[u_1(l,t), \ldots, u_M(l,t)]^{\mathrm{T}} + \mathbf{w}(l,t) \tag{1}$$

where $\alpha_p(t)$ is the reflection coefficient depending on the radar cross section of the pth target, $u_m(l,t)$ is the signal waveform transmitted by the mth transmitting antenna, such as BPSK modulated signal waveform. $\mathbf{w}(l,t)$ is the noise vector. l and t indicate the time within pulse (fast time) and the index of radar pulse (slow time), respectively. $\tilde{\mathbf{a}}_t(\theta_p) = \mathbf{G}_t\boldsymbol{\Phi}_t\mathbf{a}_t(\theta_p)$, and $\tilde{\mathbf{a}}_r(\theta_p) = \mathbf{G}_r\boldsymbol{\Phi}_r\mathbf{a}_r(\theta_p)$, $p = 1, 2, \ldots P$. Furthermore, $\mathbf{a}_t(\theta_p) = [1, e^{j\pi\sin(\theta_p)}, e^{j\pi 2\sin(\theta_p)}, \ldots, e^{j\pi(M-1)\sin(\theta_p)}]^{\mathrm{T}}$ and $\mathbf{a}_r(\theta_p) = [1, e^{j\pi\sin(\theta_p)}, e^{j\pi 2\sin(\theta_p)}, \ldots, e^{j\pi(N-1)\sin(\theta_p)}]^{\mathrm{T}}$

are transmit and receive steering vectors, respectively. $\mathbf{G}_t = \text{diag}(\rho_{t1}, \rho_{t2}, \ldots, \rho_{tM})$ and $\boldsymbol{\Phi}_t = \text{diag}(e^{j\varphi_{t1}}, e^{j\varphi_{t2}}, \ldots, e^{j\varphi_{tM}})$ with ρ_{tm} and φ_{tm} respectively being the gain and the phase errors of the mth antenna in transmit array. Similarly, $\mathbf{G}_r = \text{diag}(\rho_{r1}, \rho_{r2}, \ldots, \rho_{rN})$ and $\boldsymbol{\Phi}_r = \text{diag}(e^{j\varphi_{r1}}, e^{j\varphi_{r2}}, \ldots, e^{j\varphi_{rN}})$ with ρ_{rn} and φ_{rn} respectively being the gain and the phase errors of the nth antenna at the receive array. For well-calibrated antennas, i.e. the antennas corresponding to the subarray that can be considered without gain or phase errors, the corresponding error entries in $\mathbf{G}_t$, $\boldsymbol{\Phi}_t$, $\mathbf{G}_r$ and $\boldsymbol{\Phi}_r$, are replaced by $\rho_{t\bar{m}} = e^{j\varphi_{t\bar{m}}} = 1$ with $\bar{m} = 1, 2 \ldots M_c$, and $\rho_{r\bar{n}} = e^{j\varphi_{r\bar{n}}} = 1$ with $\bar{n} = 1, 2 \ldots N_c$ [33,34]. Here, M_c and N_c denote the numbers of well-calibrated antennas in transmit and receive arrays, respectively, and it is assumed that $c = \min\{M_c, N_c\} > 1$ [20–22]. By matched filtering on $\mathbf{x}(l, t)$ in Eq. (1), the complex envelope of the output of the mth carrier matched filter can be expressed as [27–32]

$$\begin{aligned} \mathbf{x}_m(t) &= \sum_{p=1}^{P} \alpha_p(t) \tilde{\mathbf{a}}_r(\theta_p) \tilde{\mathbf{a}}_t^{\mathrm{T}}(\theta_p) \gamma(t) [\underbrace{0, \ldots, 0}_{m-1}, 1, \underbrace{0, \ldots, 0}_{M-m}]^{\mathrm{T}} + \mathbf{w}_m(t) \\ &= \sum_{p=1}^{P} \tilde{\mathbf{a}}_r(\theta_p) \tilde{\mathbf{a}}_{tm}^{\mathrm{T}}(\theta_p) s_p(t) + \mathbf{w}_m(t) \end{aligned} \tag{2}$$

where $\tilde{\mathbf{a}}_{tm}$ is the mth element of $\tilde{\mathbf{a}}_t$, $\gamma(t)$ is the baseband signal transmitted by the transmitter, such as non-circular signal, and $s_p(t) = \alpha_p(t)\gamma(t)$ with the target reflection gain $\alpha_p(t)$. $\mathbf{w}_m(t)$ is the noise vector after the mth matched filter. Let $\mathbf{x}(t) \in \mathbb{C}^{MN\times 1}$ be the output after all the matched filters, the received data vector is written as

$$\begin{aligned} \mathbf{x}(t) &= \text{vec}([\mathbf{x}_1^{\mathrm{T}}(t), \ldots, \mathbf{x}_M^{\mathrm{T}}(t)]^{\mathrm{T}}) \\ &= \tilde{\mathbf{A}}\mathbf{s}(t) + \mathbf{n}(t) \end{aligned} \tag{3}$$

where $\mathbf{x}(t) \in \mathbb{C}^{MN\times 1}$, $\mathbf{s}(t) = [s_1(t), s_2(t), \ldots, s_P(t)]^{\mathrm{T}} \in \mathbb{C}^{P\times 1}$ is the reflected signal vector after the carrier matched filters. $\mathbf{n}(t) = [\mathbf{w}_1^{\mathrm{T}}(t), \ldots, \mathbf{w}_M^{\mathrm{T}}(t)]^{\mathrm{T}} \in \mathbb{C}^{MN\times 1}$ is the white or colored Gaussian noise vector, and $\tilde{\mathbf{A}}$ is the uncalibrated transmit-receive steering matrix with gain-phase errors. $\tilde{\mathbf{A}}$ is represented as [20–22]

$$\begin{aligned} \tilde{\mathbf{A}} &= [\mathbf{G}_t\boldsymbol{\Phi}_t\mathbf{a}_t(\theta_1) \otimes \mathbf{G}_r\boldsymbol{\Phi}_r\mathbf{a}_r(\theta_1), \ldots, \mathbf{G}_t\boldsymbol{\Phi}_t\mathbf{a}_t(\theta_P) \otimes \mathbf{G}_r\boldsymbol{\Phi}_r\mathbf{a}_r(\theta_P)] \\ &= \tilde{\mathbf{A}}_t \odot \tilde{\mathbf{A}}_r \end{aligned} \tag{4}$$

where $\tilde{\mathbf{A}} \in \mathbb{C}^{MN\times P}$, $\tilde{\mathbf{A}}_t = [\tilde{\mathbf{a}}_t(\theta_1), \tilde{\mathbf{a}}_t(\theta_2), \ldots, \tilde{\mathbf{a}}_t(\theta_P)] \in \mathbb{C}^{M\times P}$, and $\tilde{\mathbf{A}}_r = [\tilde{\mathbf{a}}_r(\theta_1), \tilde{\mathbf{a}}_r(\theta_2), \ldots, \tilde{\mathbf{a}}_r(\theta_P)] \in \mathbb{C}^{N\times P}$. $\tilde{\mathbf{A}}$ can be expressed as $\tilde{\mathbf{A}} = [\tilde{\mathbf{a}}(\theta_1), \tilde{\mathbf{a}}(\theta_2), \ldots, \tilde{\mathbf{a}}(\theta_P)]$, and $\tilde{\mathbf{a}}(\theta_p)$ satisfies

$$\begin{aligned} \tilde{\mathbf{a}}(\theta_p) &= \mathbf{G}_t\boldsymbol{\Phi}_t\mathbf{a}_t(\theta_p) \otimes \mathbf{G}_r\boldsymbol{\Phi}_r\mathbf{a}_r(\theta_p) \\ &= \tilde{\mathbf{a}}_t(\theta_p) \otimes \tilde{\mathbf{a}}_r(\theta_p) \end{aligned} \tag{5}$$

where $p = 1, 2, \ldots P$. Consequently, the received data in Eq. (3) can be rewritten as [17,33,34]

$$\begin{aligned} \mathbf{x}(t) &= [\mathbf{G}_t\boldsymbol{\Phi}_t \otimes \mathbf{G}_r\boldsymbol{\Phi}_r][\mathbf{a}(\theta_1), \ldots, \mathbf{a}(\theta_P)]\mathbf{s}(t) + \mathbf{n}(t) \\ &= \boldsymbol{\Gamma}\mathbf{A}\mathbf{s}(t) + \mathbf{n}(t) \end{aligned} \tag{6}$$

where gain-phase error matrix $\boldsymbol{\Gamma} = (\mathbf{G}_t\boldsymbol{\Phi}_t \otimes \mathbf{G}_r\boldsymbol{\Phi}_r) \in \mathbb{C}^{MN\times MN}$ is a diagonal matrix, which contains the information of the gain-phase errors in both arrays. $\mathbf{A} = [\mathbf{a}(\theta_1), \mathbf{a}(\theta_2), \ldots, \mathbf{a}(\theta_P)] \in \mathbb{C}^{MN\times P}$ with $\mathbf{a}(\theta_p) = \mathbf{a}_t(\theta_p) \otimes \mathbf{a}_r(\theta_p)$, $p = 1, 2, \ldots P$ being the steering vector. As in [25], we introduce three assumptions regarding the noises and the signals.

1. The noises in $\mathbf{n}(t)$ are Gaussian with zero-mean, and may be colored and spatially correlated.
2. The signals in $\mathbf{s}(t)$ are non-Gaussian with zero-mean and statistically independent with each other.
3. The noises in $\mathbf{n}(t)$ are independent with the signals in $\mathbf{s}(t)$.

According to the structure of the received data vector $\mathbf{x}(t)$ with gain-phase errors in Eq. (6), in order to achieve the DOA estimation for both white and colored Gaussian noise conditions, FOC-based sparse representation cannot be directly applied to estimate the DOAs due to the unknown gain-phase error matrix $\boldsymbol{\Gamma}$. Otherwise, jointly optimizing $\boldsymbol{\Gamma}$ and the angles brings in a complex nonconvex optimization problem, which is hard to solve. In the following, for DOA estimation in the presence of gain-phase errors, an efficient sparse algorithm with fourth-order cumulants based error matrix estimation is proposed for MIMO radar.

3. FOC-based sparse DOA estimation algorithm for MIMO radar with gain-phase errors

3.1. Gain-phase error estimation

To use the high-order cumulants to estimate the gain-phase error matrix, firstly, we define the fourth-order cumulant $c_x(k_1, k_2, k_3, k_4)$ of data $\mathbf{x}$ with J snapshots as the following form

$$\begin{aligned} \text{cum}\{\mathbf{x}_{k_1}, \mathbf{x}_{k_2}^*, \mathbf{x}_{k_3}, \mathbf{x}_{k_4}^*\} = {} & \text{E}(\mathbf{x}_{k_1}\mathbf{x}_{k_2}^*\mathbf{x}_{k_3}\mathbf{x}_{k_4}^*) - \text{E}(\mathbf{x}_{k_1}\mathbf{x}_{k_2}^*)\text{E}(\mathbf{x}_{k_3}\mathbf{x}_{k_4}^*) \\ & - \text{E}(\mathbf{x}_{k_1}\mathbf{x}_{k_3})\text{E}(\mathbf{x}_{k_2}^*\mathbf{x}_{k_4}^*) - \text{E}(\mathbf{x}_{k_1}\mathbf{x}_{k_4}^*)\text{E}(\mathbf{x}_{k_2}^*\mathbf{x}_{k_3}) \end{aligned} \tag{7}$$

where $\mathbf{x}_{k_i}$ is the k_ith element in $\mathbf{x}$, $1 \le k_i \le MN$, $i = 1, 2, 3, 4$. In fact each term in $c_x(k_1, k_2, k_3, k_4)$ is estimated from

$$\begin{aligned}\mathrm{E}(\mathbf{x}_{k_1}\mathbf{x}^*_{k_2}\mathbf{x}_{k_3}\mathbf{x}^*_{k_4}) &\approx \frac{1}{J}\sum_{t=1}^{J}\mathbf{x}_{k_1}(t)\mathbf{x}^*_{k_2}(t)\mathbf{x}_{k_3}(t)\mathbf{x}^*_{k_4}(t)\\ \mathrm{E}(\mathbf{x}_{k_1}\mathbf{x}^*_{k_2}) &\approx \frac{1}{J}\sum_{t=1}^{J}\mathbf{x}_{k_1}(t)\mathbf{x}^*_{k_2}(t)\end{aligned} \tag{8}$$

where J is the number of snapshots. Based on Eq. (7) and Eq. (8), making full use of the specialty of fourth-order cumulants obtained from all possible permutations of indices (k_1, k_2, k_3, k_4) and the well-calibrated parts of steering vectors, firstly, the gain errors can be extracted from the gain-phase errors into an orderly matrix $\mathbf{M}_\rho \in \mathbb{C}^{N\times M}$, with its (k_1, k_2)th element designed as

$$\begin{aligned}\mathbf{M}_\rho(k_1,k_2) &= \mathrm{cum}\{\mathbf{x}_{(k_2-1)N+k_1}, \mathbf{x}_1{}^*, \mathbf{x}_1, \mathbf{x}^*_{(k_2-1)N+k_1}\}\\ &= \sum_{p=1}^{P}\tilde{\mathbf{a}}_{(k_2-1)N+k_1}(\theta_p)\tilde{\mathbf{a}}^*_{(k_2-1)N+k_1}(\theta_p)\beta_p|\tilde{\mathbf{a}}^*_1(\theta_p)|^2\end{aligned} \tag{9}$$

with the assumptions about the noises and the signals. In Eq. (9), $1 \le k_1 \le N$, $1 \le k_2 \le M$, $\tilde{\mathbf{a}}_k(\theta_p)$ is the kth item of $\tilde{\mathbf{a}}(\theta_p)$, and $\beta_p = \mathrm{cum}(s_p, s^*_p, s_p, s^*_p)$ is the fourth-order cumulant of s_p. Thus on the basis of the definition of $\tilde{\mathbf{a}}(\theta_p)$ in Eq. (5), let $e^{j\vartheta_p} = \mathbf{a}_{tk_2}(\theta_p)\mathbf{a}_{rk_1}(\theta_p) = e^{j\pi(k_1+k_2-2)\sin(\theta_p)}$ with $\mathbf{a}_{tk_2}(\theta_p)$ and $\mathbf{a}_{rk_1}(\theta_p)$ being the k_2th and the k_1th elements in $\mathbf{a}_t(\theta_p)$ and $\mathbf{a}_r(\theta_p)$, we can derive that

$$\begin{aligned}\mathbf{M}_\rho(k_1,k_2) &= \sum_{p=1}^{P}\rho_{tk_2}\rho_{rk_1}e^{j(\varphi_{tk_2}+\varphi_{rk_1})+j\vartheta_p}(\rho_{tk_2}\rho_{rk_1}e^{j(\varphi_{tk_2}+\varphi_{rk_1})+j\vartheta_p})^*\beta_p\\ &= \sum_{p=1}^{P}\beta_p\rho^2_{rk_1}\rho^2_{tk_2}\end{aligned} \tag{10}$$

As a result, the proposed fourth-order cumulants based gain error matrix $\mathbf{M}_\rho$ is in the following form

$$\begin{aligned}\mathbf{M}_\rho &= \sum_{p=1}^{P}\beta_p\begin{bmatrix}\rho^2_{r1}\rho^2_{t1} & \rho^2_{r1}\rho^2_{t2} & \cdots & \rho^2_{r1}\rho^2_{tM}\\ \rho^2_{r2}\rho^2_{t1} & \rho^2_{r2}\rho^2_{t2} & \cdots & \rho^2_{r2}\rho^2_{tM}\\ \vdots & \vdots & \ddots & \vdots\\ \rho^2_{rN}\rho^2_{t1} & \rho^2_{rN}\rho^2_{t2} & \cdots & \rho^2_{rN}\rho^2_{tM}\end{bmatrix}\\ &= (\sum_{p=1}^{P}\beta_p)[\rho^2_{r1}, \rho^2_{r2}, \ldots, \rho^2_{rN}]^{\mathrm{T}}[\rho^2_{t1}, \rho^2_{t2}, \ldots, \rho^2_{tM}]\end{aligned} \tag{11}$$

Then exploiting the matrix structure of $\mathbf{M}_\rho$, ρ^2_{ri} and ρ^2_{tj} can be obtained from

$$\begin{aligned}\rho^2_{ri} &= \frac{1}{M}\sum_{k_2=1}^{M}\{\mathbf{M}_\rho(i,k_2)/[\frac{1}{N_c}\sum_{k_1=1}^{N_c}\mathbf{M}_\rho(k_1,k_2)]\}\\ \rho^2_{tj} &= \frac{1}{N}\sum_{k_1=1}^{N}\{\mathbf{M}_\rho(k_1,j)/[\frac{1}{M_c}\sum_{k_2=1}^{M_c}\mathbf{M}_\rho(k_1,k_2)]\}\end{aligned} \tag{12}$$

for $i = N_c + 1, \ldots, N$, and $j = M_c + 1, \ldots, M$. After estimating the gain errors ρ_{ri} and ρ_{tj}, based on Eq. (7) and Eq. (8), we further construct an FOC-based error matrix $\mathbf{M}_{\varphi r} \in \mathbb{C}^{(N-1)\times M}$ to derive the phase errors at the receive array, with its (k_1, k_2)th entry designed as

$$\begin{aligned}\mathbf{M}_{\varphi r}(k_1,k_2) &= \mathrm{cum}\{\mathbf{x}_{(k_2-1)N+k_1+1}, \mathbf{x}_1{}^*, \mathbf{x}_1, \mathbf{x}^*_{(k_2-1)N+k_1}\}\\ &= (\tilde{\mathbf{A}}_{r(k_1+1)}\odot\tilde{\mathbf{A}}_{tk_2})\mathbf{C}_s(\tilde{\mathbf{A}}_{rk_1}\odot\tilde{\mathbf{A}}_{tk_2})^{\mathrm{H}}\\ &= \varpi\rho^2_{tk_2}\rho_{r(k_1+1)}\rho_{rk_1}e^{j\varphi_{r(k_1+1)}-j\varphi_{rk_1}}\end{aligned} \tag{13}$$

where $\mathbf{C}_s = \mathrm{diag}(\beta_1, \beta_2, \ldots, \beta_P) \in \mathbb{C}^{P\times P}$ is the fourth-order cumulant matrix of s_p with $p = 1, 2, \ldots P$. $\varpi = \sum_{p=1}^{P}e^{j\pi\sin(\theta_p)}\beta_p$, $1 \le k_1 \le N-1$ and $1 \le k_2 \le M$. $\tilde{\mathbf{A}}_{rk}$ and $\tilde{\mathbf{A}}_{tk}$ are the kth rows in $\tilde{\mathbf{A}}_r$ and $\tilde{\mathbf{A}}_t$, respectively. To make it explicitly show the structure regularity of the designed FOC-based error matrix $\mathbf{M}_{\varphi r}$, we express $\mathbf{M}_{\varphi r}$ in detail as follows

$$\mathbf{M}_{\varphi r} = \varpi\begin{bmatrix}\rho^2_{t1}\rho_{r2}\rho_{r1}e^{j\varphi_{r2}-j\varphi_{r1}} & \rho^2_{t2}\rho_{r2}\rho_{r1}e^{j\varphi_{r2}-j\varphi_{r1}} & \cdots & \rho^2_{tM}\rho_{r2}\rho_{r1}e^{j\varphi_{r2}-j\varphi_{r1}}\\ \rho^2_{t1}\rho_{r3}\rho_{r2}e^{j\varphi_{r3}-j\varphi_{r2}} & \rho^2_{t2}\rho_{r3}\rho_{r2}e^{j\varphi_{r3}-j\varphi_{r2}} & \cdots & \rho^2_{tM}\rho_{r3}\rho_{r2}e^{j\varphi_{r3}-j\varphi_{r2}}\\ \rho^2_{t1}\rho_{r4}\rho_{r3}e^{j\varphi_{r4}-j\varphi_{r3}} & \rho^2_{t2}\rho_{r4}\rho_{r3}e^{j\varphi_{r4}-j\varphi_{r3}} & \cdots & \rho^2_{tM}\rho_{r4}\rho_{r3}e^{j\varphi_{r4}-j\varphi_{r3}}\\ \vdots & \vdots & \ddots & \vdots\\ \rho^2_{t1}\rho_{rN}\rho_{r(N-1)}e^{j\varphi_{rN}-j\varphi_{r(N-1)}} & \rho^2_{t2}\rho_{rN}\rho_{r(N-1)}e^{j\varphi_{rN}-j\varphi_{r(N-1)}} & \cdots & \rho^2_{tM}\rho_{rN}\rho_{r(N-1)}e^{j\varphi_{rN}-j\varphi_{r(N-1)}}\end{bmatrix} \tag{14}$$

It can be observed in Eq. (14) that $\mathbf{M}_{\varphi r}(1,k_2)=\ldots=\mathbf{M}_{\varphi r}(N_c-1,k_2)=\varpi\rho_{tk_2}^2$ for $k_2=1,2,\ldots,M$. With regard to the phase errors, $\mathbf{M}_{\varphi r}(k_1,k_2)$ just contains $e^{j\varphi_{r(k_1+1)}}$ and $e^{j\varphi_{rk_1}}$. As a result, utilizing the continuous multiplication operator, $\rho_{ri}e^{j\varphi_{ri}}$ is derived as

$$\rho_{ri}e^{j\varphi_{ri}}=\frac{\rho_{ri}^2}{M}\sum_{k_2=1}^{M}[(\prod_{k_1=1}^{i-1}\frac{\mathbf{M}_{\varphi r}(k_1,k_2)}{\rho_{r(k_1+1)}^2})/\varepsilon_{k_2}^{i-1}] \tag{15}$$

where $\varepsilon_{k_2}=\frac{1}{N_c-1}\sum_{k_1=1}^{N_c-1}\mathbf{M}_{\varphi r}(k_1,k_2)$, and $i=N_c+1,\ldots,N$. In each element of the designed FOC-based error matrix $\mathbf{M}_{\varphi r}$, $\rho_{r(k_1+1)}\rho_{rk_1}e^{j\varphi_{r(k_1+1)}-j\varphi_{rk_1}}$ does not depend on the value of k_2. Taking the average of $\rho_{ri}e^{j\varphi_{ri}}$ and $\varpi\rho_{tk_2}^2$ from all columns in $\mathbf{M}_{\varphi r}$ and all the first N_c-1 rows in $\mathbf{M}_{\varphi r}(:,k_2)$, guarantees the gain-phase error estimation to be less affected by FOC estimation errors. After estimating the gain-phase errors of the receive array, another FOC-based error matrix $\mathbf{M}_{\varphi t}\in\mathbb{C}^{(M-1)\times N}$ regarding the phase errors of the transmitter is designed as follows

$$\begin{aligned}\mathbf{M}_{\varphi t}(k_1,k_2)&=\mathrm{cum}\{\mathbf{x}_{k_1N+k_2},\mathbf{x}_1{}^*,\mathbf{x}_1,\mathbf{x}^*_{(k_1-1)N+k_2}\}\\&=(\tilde{\mathbf{A}}_{t(k_1+1)}\odot\tilde{\mathbf{A}}_{rk_2})\mathbf{C}_s(\tilde{\mathbf{A}}_{tk_1}\odot\tilde{\mathbf{A}}_{rk_2})^{\mathrm{H}}\\&=\varpi\rho_{rk_2}^2\rho_{t(k_1+1)}\rho_{tk_1}e^{j\varphi_{t(k_1+1)}-j\varphi_{tk_1}}\end{aligned} \tag{16}$$

where $1\le k_1\le M-1$ and $1\le k_2\le N$. Consequently, with respect to the errors of the transmit array, the proposed fourth-order cumulants based error matrix $\mathbf{M}_{\varphi t}$ is written as

$$\mathbf{M}_{\varphi t}=\varpi\begin{bmatrix}\rho_{r1}^2\rho_{t2}\rho_{t1}e^{j\varphi_{t2}-j\varphi_{t1}} & \rho_{r2}^2\rho_{t2}\rho_{t1}e^{j\varphi_{t2}-j\varphi_{t1}} & \cdots & \rho_{rN}^2\rho_{t2}\rho_{t1}e^{j\varphi_{t2}-j\varphi_{t1}}\\ \rho_{r1}^2\rho_{t3}\rho_{t2}e^{j\varphi_{t3}-j\varphi_{t2}} & \rho_{r2}^2\rho_{t3}\rho_{t2}e^{j\varphi_{t3}-j\varphi_{t2}} & \cdots & \rho_{rN}^2\rho_{t3}\rho_{t2}e^{j\varphi_{t3}-j\varphi_{t2}}\\ \rho_{r1}^2\rho_{t4}\rho_{t3}e^{j\varphi_{t4}-j\varphi_{t3}} & \rho_{r2}^2\rho_{t4}\rho_{t3}e^{j\varphi_{t4}-j\varphi_{t3}} & \cdots & \rho_{rN}^2\rho_{t4}\rho_{t3}e^{j\varphi_{t4}-j\varphi_{t3}}\\ \vdots & \vdots & \ddots & \vdots\\ \rho_{r1}^2\rho_{tM}\rho_{t(M-1)}e^{j\varphi_{tM}-j\varphi_{t(M-1)}} & \rho_{r2}^2\rho_{tM}\rho_{t(M-1)}e^{j\varphi_{tM}-j\varphi_{t(M-1)}} & \cdots & \rho_{rN}^2\rho_{tM}\rho_{t(M-1)}e^{j\varphi_{tM}-j\varphi_{t(M-1)}}\end{bmatrix} \tag{17}$$

Similar to Eq. (15), based on the matrix structure of $\mathbf{M}_{\varphi t}$, it results in

$$\rho_{tj}e^{j\varphi_{tj}}=\frac{\rho_{tj}^2}{N}\sum_{k_2=1}^{N}[(\prod_{k_1=1}^{j-1}\frac{\mathbf{M}_{\varphi t}(k_1,k_2)}{\rho_{t(k_1+1)}^2})/\tilde{\varepsilon}_{k_2}^{j-1}] \tag{18}$$

where $\tilde{\varepsilon}_{k_2}=\frac{1}{M_c-1}\sum_{k_1=1}^{M_c-1}\mathbf{M}_{\varphi t}(k_1,k_2)$, and $j=M_c+1,\ldots,M$. With $\rho_{ri}e^{j\varphi_{ri}}$ and $\rho_{tj}e^{j\varphi_{tj}}$, the gain-phase error matrix $\mathbf{\Gamma}$ can be calculated by Kronecker product operator, that is

$$\mathbf{\Gamma}=[\mathrm{diag}(\rho_{t1}e^{j\varphi_{t1}},\ldots,\rho_{tM}e^{j\varphi_{tM}})]\otimes[\mathrm{diag}(\rho_{r1}e^{j\varphi_{r1}},\ldots,\rho_{rN}e^{j\varphi_{rN}})] \tag{19}$$

3.2. Dimensional reduction for error matrix and received data

Although the gain-phase errors are obtained, for the current forms of the error matrix $\mathbf{\Gamma}$ in Eq. (19) and the received data $\mathbf{x}(t)$ in Eq. (6), the following FOC operation will lead to tremendous calculation burden and then the difficult sparse signal reconstruction. Next, we introduce the transformation to reduce the dimension of $\mathbf{\Gamma}$ and $\mathbf{x}(t)$. Let $z_p=e^{j\pi\sin(\theta_p)}$, $p=1,2,\ldots,P$, the detailed representation of the column $\mathbf{a}_t(\theta_p)\otimes\mathbf{a}_r(\theta_p)\in\mathbb{C}^{MN\times 1}$ in $\mathbf{A}$ is

$$\mathbf{a}(\theta_p)=(1,\ldots,z_p^{N-1},z_p,\ldots,z_p^{N},\ldots,z_p^{M-1},\ldots,z_p^{M+N-2})^{\mathrm{T}} \tag{20}$$

Then $\tilde{\mathbf{a}}(\theta_p)$ can be represented as follows

$$\tilde{\mathbf{a}}(\theta_p)=\mathbf{\Gamma}\mathbf{G}\mathbf{b}(\theta_p) \tag{21}$$

where $\mathbf{b}(\theta_p)=[1,e^{j\pi\sin(\theta_p)},\cdots,e^{j\pi(M+N-2)\sin(\theta_p)}]^{\mathrm{T}}\in\mathbb{C}^{(M+N-1)\times 1}$, $\mathbf{G}=[\mathbf{L}_0^{\mathrm{T}},\mathbf{L}_1^{\mathrm{T}},\cdots,\mathbf{L}_{M-1}^{\mathrm{T}}]^{\mathrm{T}}\in\mathbb{C}^{MN\times(M+N-1)}$ with $\mathbf{L}_m=[\mathbf{0}_{N\times m},\mathbf{I}_N,\mathbf{0}_{N\times(M-m-1)}]\in\mathbb{C}^{N\times(M+N-1)}$, $m=0,1,...,M-1$. Hence, let $\tilde{\mathbf{J}}=(\mathbf{G}^{\mathrm{H}}\mathbf{G})^{(-\frac{1}{2})}\mathbf{G}^{\mathrm{H}}$ be the reduced dimensional matrix, at the same time, $\mathbf{F}=(\mathbf{G}^{\mathrm{H}}\mathbf{G})^{(\frac{1}{2})}$ can be calculated as

$$\mathbf{F}=\mathrm{diag}[1,\sqrt{2},...,\underbrace{\min(\sqrt{M},\sqrt{N}),...,\min(\sqrt{M},\sqrt{N})}_{|M-N|+1},....,\sqrt{2},1] \tag{22}$$

When we use $\tilde{\mathbf{J}}$ to carry out the reduced dimensional transformation, the noises can remain Gaussian because of the invariance speciality of linear transformation. Thus multiplying $\tilde{\mathbf{J}}$ on the left side of $\mathbf{x}(t)$ in Eq. (6), the new data vector $\tilde{\mathbf{x}}(t)$ is

$$\begin{aligned}\tilde{\mathbf{x}}(t)&=\tilde{\mathbf{J}}\mathbf{\Gamma}\mathbf{G}\mathbf{B}\mathbf{s}(t)+\tilde{\mathbf{J}}\mathbf{n}(t)\\&=(\mathbf{G}^{\mathrm{H}}\mathbf{G})^{(-\frac{1}{2})}\mathbf{G}^{\mathrm{H}}(\mathbf{G}\mathbf{G}^{+})\mathbf{\Gamma}\mathbf{G}\mathbf{B}\mathbf{s}(t)+\tilde{\mathbf{n}}(t)\\&=\mathbf{F}\tilde{\mathbf{\Gamma}}\mathbf{B}\mathbf{s}(t)+\tilde{\mathbf{n}}(t)\end{aligned} \tag{23}$$

where $(\cdot)^+$ denotes pseudo-inverse operator, $\mathbf{B} = [\mathbf{b}(\theta_1), \mathbf{b}(\theta_2), \ldots, \mathbf{b}(\theta_P)] \in \mathbb{C}^{(M+N-1)\times P}$ and $\tilde{\mathbf{n}}(t) \in \mathbb{C}^{(M+N-1)\times 1}$ are the new transmit-receive steering matrix and Gaussian noise vector, respectively. Meanwhile, in Eq. (23), $\tilde{\boldsymbol{\Gamma}}$ that contains $\mathbf{G}$ and $\mathbf{G}^+$ is derived as

$$\tilde{\boldsymbol{\Gamma}} = \mathbf{G}^+ \boldsymbol{\Gamma} \mathbf{G} \tag{24}$$

where $\mathbf{G}^+ = (\mathbf{G}^{\mathrm{T}}\mathbf{G})^{-1}\mathbf{G}^{\mathrm{T}} \in \mathbb{C}^{(M+N-1)\times MN}$, and $\tilde{\boldsymbol{\Gamma}}$ is a new gain-phase error matrix with a low dimension. $\tilde{\boldsymbol{\Gamma}} \in \mathbb{C}^{(M+N-1)\times(M+N-1)}$ is based on $\boldsymbol{\Gamma} \in \mathbb{C}^{MN\times MN}$ which is obtained from Eq. (19). Thanks to the reduced dimensional transformation, the received data vector transforms into $\tilde{\mathbf{x}}(t) \in \mathbb{C}^{(M+N-1)\times J}$, and the dimension of the gain-phase error matrix $\boldsymbol{\Gamma}$ is reduced from $MN \times MN$ to $(M+N-1)\times(M+N-1)$.

3.3. FOC-based sparse DOA estimation in the presence of gain-phase error matrix

After obtaining the new gain-phase error matrix $\tilde{\boldsymbol{\Gamma}}$ from Eq. (19) and Eq. (24), and reducing the dimension of $\mathbf{x}$, we can calculate an FOC-based measurement matrix $\mathbf{C}_{\tilde{x}} \in \mathbb{C}^{(M+N-1)\times(M+N-1)}$, whose the (k_1,k_2)th entry is [26]

$$\mathbf{C}_{\tilde{x}}(k_1,k_2) = \mathrm{cum}\{\tilde{\mathbf{x}}_{k_1}, \tilde{\mathbf{x}}^*_{k_2}, \tilde{\mathbf{x}}_{k_2}, \tilde{\mathbf{x}}^*_{k_2}\} \tag{25}$$

When all possible permutations of k_1 and k_2 are considered in Eq. (25), the $(M+N-1)^2$ values are organized compatibly in the FOC matrix $\mathbf{C}_{\tilde{x}}$. To further reduce the computational complexity, $\mathbf{C}_{\tilde{x}}$ can be turned into [26]

$$\tilde{\mathbf{C}}_{\tilde{x}} = \mathbf{C}_{\tilde{x}}\mathbf{V}_s = \mathbf{F}\tilde{\boldsymbol{\Gamma}}\mathbf{B}\mathbf{C}_s\mathbf{S}^{\mathrm{H}}_{FB}\mathbf{V}_s \in \mathbb{C}^{(M+N-1)\times P} \tag{26}$$

where $\mathbf{S}_{FB} \in \mathbb{C}^{(M+N-1)\times P}$, whose the ith row and jth column element is $\mathbf{S}_{FB}(i,j) = |[\mathbf{F}\tilde{\boldsymbol{\Gamma}}\mathbf{b}(\theta_j)]_i|^2[\mathbf{F}\tilde{\boldsymbol{\Gamma}}\mathbf{b}(\theta_j)]_i$, $1 \le i \le (M+N-1)$, $1 \le j \le P$, and $[\mathbf{F}\tilde{\boldsymbol{\Gamma}}\mathbf{b}(\theta_j)]_i$ is the ith term in $\mathbf{F}\tilde{\boldsymbol{\Gamma}}\mathbf{b}(\theta_j)$. $\mathbf{V}_s$ is composed of the right singular vectors corresponding to the P largest singular values [26]. $\tilde{\mathbf{C}}_{\tilde{x}}$ contains the vast majority of the signal power, which is deemed to be the new measurement matrix instead of $\mathbf{C}_{\tilde{x}}$. Let $\mathbf{B}_{\hat{\theta}} = [\mathbf{b}(\hat{\theta}_1), \mathbf{b}(\hat{\theta}_2), \ldots, \mathbf{b}(\hat{\theta}_L)] \in \mathbb{C}^{(M+N-1)\times L}$ be a complete dictionary, with the discretized sample direction grid $\{\hat{\theta}_1, \hat{\theta}_2, \cdots, \hat{\theta}_L\}$, $L \gg P$. As a consequence, a reweighted l_1-norm constrained minimization sparse representation scheme can be formulated as [26]

$$\min_{\tilde{\mathbf{S}}_{\hat{\theta}}} \|\mathbf{W}_r\tilde{\mathbf{S}}^{(l_2)}_{\hat{\theta}}\|_1, \quad \text{s.t.} \|\hat{\tilde{\mathbf{C}}}_{\tilde{x}} - \mathbf{F}\hat{\tilde{\boldsymbol{\Gamma}}}\mathbf{B}_{\hat{\theta}}\tilde{\mathbf{S}}_{\hat{\theta}}\|_F \le \sqrt{\eta} \tag{27}$$

where $\hat{\tilde{\boldsymbol{\Gamma}}}$ is the estimation of the true gain-phase error matrix $\tilde{\boldsymbol{\Gamma}}$, $\hat{\tilde{\mathbf{C}}}_{\tilde{x}}$ is the sample estimation, and $[\tilde{\mathbf{S}}^{(l_2)}_{\hat{\theta}}]_i = \|\tilde{\mathbf{S}}_{\hat{\theta}}(i,:)\|_2$. Reweighted matrix $\mathbf{W}_r$ can enhance the sparse solution, and it is calculated from $\mathbf{W}_r = \mathrm{diag}[(\mathbf{W}^{(l_2)})^{\mathrm{T}}]/\max[(\mathbf{W}^{(l_2)})^{\mathrm{T}}]$ with $\mathbf{W} = (\mathbf{F}\hat{\tilde{\boldsymbol{\Gamma}}}\mathbf{B}_{\hat{\theta}})^{\mathrm{H}}\mathbf{U}_n$. η is a regularization parameter, which can be chosen as the upper limit value of asymptotic chi-square distribution with $(M+N-1)P$ freedom degrees and a high probability $1-\varepsilon$ confidence interval upon variance uniformization of the FOC estimation errors [26], and $\varepsilon = 0.001$ is enough. Eq. (27) can be solved by SOC (second order cone) programming software packages such as SeDuMi [35] and CVX [36].

Thus, substituting the estimated fourth-order cumulants based gain-phase error matrix $\hat{\tilde{\boldsymbol{\Gamma}}}$ obtained from Eq. (12), (15), (18), (19) and (24), into Eq. (27), by searching the spectrum of $\tilde{\mathbf{S}}^{(l_2)}_{\hat{\theta}}$, the DOA estimation for MIMO radar in the presence of gain-phase errors is achieved.

4. Related remarks

Remark 1: In the proposed DOA estimation algorithm with fourth-order cumulants based error matrix estimation, the main calculation burden is focused on calculating the FOC-based gain-phase errors that requires $O[MNJ + M(N-1)J + N(M-1)J]$; computing the fourth-order cumulant observation matrix, which requires $O[(M+N-1)^2J]$; obtaining the sparse solution from Eq. (27) with $O[(LP)^3]$, where L is the total number of the direction grid cells. In fact, for the designed error matrices, the applications of the advantageous fourth-order cumulant calculation formation and the dimensional reduction simplify the complexity greatly. By comparison, adaptive-SR method [16] with $\bar{Z}$ iterations costs $O[L^3J\bar{Z}]$, where l_1-norm minimization problem is solved at each snapshot separately. Thus, the proposed method has more reasonable computational complexity than adaptive-SR algorithm. For the subspace-based DOA estimation methods in the presence of gain-phase errors, RD-MUSIC algorithm [22] and ESPRIT-based algorithm [21] need about $O[(MN)^2J + (MN)^3]$ and $O[2M^2J + 2N^2J + M^3 + N^3]$ computational burden, respectively. Although the proposed algorithm has higher computational complexity than the RD-MUSIC and ESPRIT-based methods, it can provide better angle estimation performance for both white and colored Gaussian noises.

Remark 2: In the proposed method, the number of targets P is supposed to be known. The prior knowledge of P can be obtained by the minimum description length (MDL) and Akaike information criterion (AIC) principles [37]. And with respect to the maximal number of identified targets P_{max}, as discussed in [26,38,39], we can deduce that a sufficient condition for determining unique P-sparse vectors in $\tilde{\mathbf{C}}_{\tilde{x}} = \mathbf{F}\tilde{\boldsymbol{\Gamma}}\mathbf{B}_{\hat{\theta}}\mathbf{S}_{\hat{\theta}}$ is $P < [\mathrm{Spark}(\mathbf{F}\tilde{\boldsymbol{\Gamma}}\mathbf{B}_{\hat{\theta}}) - 1 + \mathrm{rank}(\tilde{\mathbf{C}}_{\tilde{x}})]/2$, where $\mathrm{Spark}(\cdot)$ is the smallest number of the linearly dependent columns. Since all of the diagonal elements in the gain-phase error matrix $\tilde{\boldsymbol{\Gamma}}$ are non-zero and $\tilde{\boldsymbol{\Gamma}}$ is nonsingular, $\mathrm{Spark}(\mathbf{F}\tilde{\boldsymbol{\Gamma}}\mathbf{B}_{\hat{\theta}}) = \mathrm{Spark}(\mathbf{B}_{\hat{\theta}})$, which indicates that $P_{max} = M + N - 2$ in the proposed method.

Remark 3: Gain-phase errors are caused by the inconsistency of the amplifier gain of the channels, and they are direction-independent [17]. This means that DOD and DOA have no impact on the errors. For different arrays of the transmitter and the receiver, the unequable inconsistency of the amplifier gain leads to different gain-phase errors [40]. As a result, the gain-phase error matrix is different for transmit and receive arrays for monostatic MIMO radar as well as bistatic MIMO radar systems.

Remark 4: In practical applications, partly-calibrated arrays, which are not fully calibrated but a portion of the antennas may be well-calibrated, are common [33]. For a partly-calibrated array, the first antenna is the reference one, thus it is considered calibrated well. In general cases, it is assumed that the antennas from the starting of the array are calibrated, whereas the last antennas are uncalibrated and exist some errors [20–22]. In the proposed method, we let the first M_c and N_c antennas of the arrays be well-calibrated, and the last $M - M_c$ and $N - N_c$ antennas be uncalibrated with uncertainties. In addition, without loss of generality, we assume that $M_c \ge 2$ and

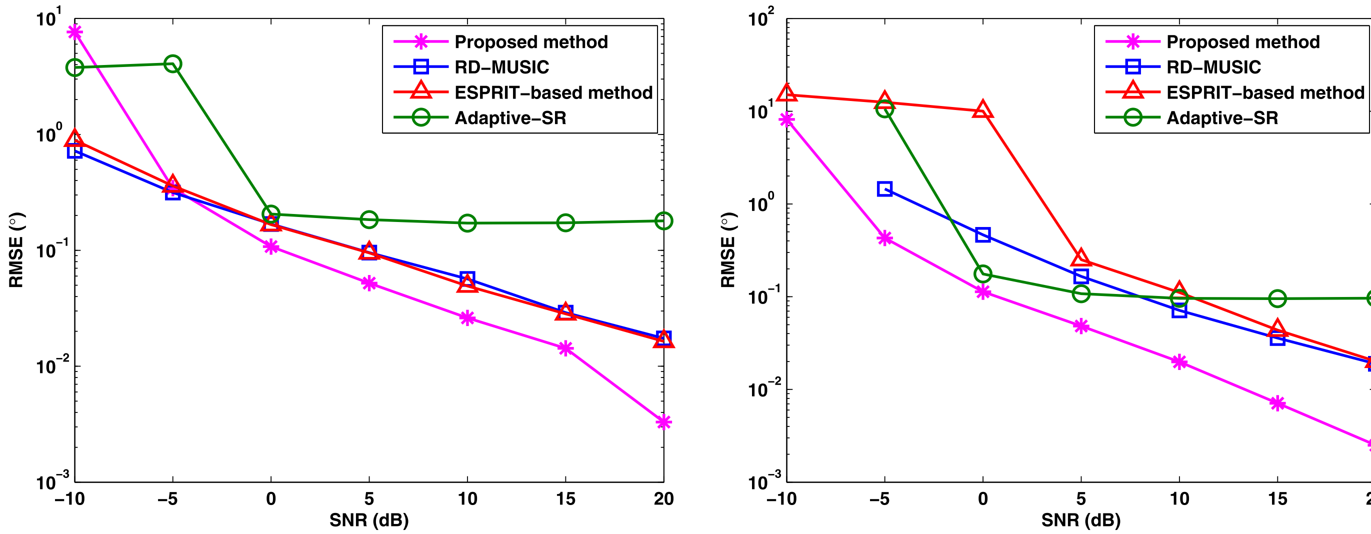

(a) white noise

(b) colored noise

Fig. 1. RMSE versus SNR with three targets.

$N_c \geq 2$ [17,33,34]. In this case, the proposed method uses all the well-calibrated antennas to estimate the gain-phase errors. The proposed DOA estimation algorithm for MIMO radar in the presence of gain-phase errors is only suitable for the partly-calibrated uniform linear arrays with $c = \min\{M_c, N_c\} > 1$.

5. Simulation results

In this section, using ESPRIT-based algorithm [21], RD-MUSIC algorithm [22] and adaptive-SR algorithm [16] for comparison, we present some simulation results to demonstrate the effectiveness and advantages of the proposed method. The root mean square error (RMSE) is used for DOA estimation performance evaluation, which is defined as

$$\mathrm{RMSE} = \sqrt{\frac{1}{PQ}\sum\nolimits_{p=1}^{P}\sum\nolimits_{i=1}^{Q}(\hat{\theta}_{p,i}-\theta_p)^2} \tag{28}$$

where $\hat{\theta}_{p,i}$ is the estimator of DOA θ_p for the ith Monte Carlo trial, Q is the number of Monte Carlo trials, $Q = 500$ and $M = N = 7$ are adopted. Gaussian noises and gain-phase errors in both transmit array and receive array are considered. In the simulations the transmitted signal is assumed binary phase shift keying (BPSK) modulated, which is widely used in practical radar systems [29–32,41]. More specifically, if the corresponding simulations involve colored noise, it is zero-mean complex Gaussian, whose covariance matrix is generated by

$$\mathbf{R}(k_1, k_2) = \sigma_n^2 r_c^{|k_1-k_2|} e^{j\pi(k_1-k_2)/2} \tag{29}$$

where σ_n^2 is power level that can be adjusted to provide the desired SNR, r_c is regression coefficient that adjusts the spatial correlation between noises, $0 < r_c \leq 1$. $\sigma_n^2 = 1$, $M_c = N_c = 2$ and $r_c = 0.7$ are considered except for the simulations with special statements, and the same values with M_c and N_c are used as the well-calibrated antenna numbers during the implementation process of RD-MUSIC and the proposed method. Moreover, gain and phase errors corresponding to the jth transmit and the ith receive antennas are respectively generated by $\rho_{tj} = 1 + e_{t\rho}\zeta_1$, $\varphi_{tj} = e_{t\varphi}\zeta_2$, $\rho_{ri} = 1 + e_{r\rho}\zeta_3$ and $\varphi_{ri} = e_{r\varphi}\zeta_4$ [16], in which $j = M_c + 1, \ldots, M$, $i = N_c + 1, \ldots, N$, ζ_1, ζ_2, ζ_3 and ζ_4 are independent and identically distributed random variables in the uniform distribution over $[-0.5, 0.5]$, and $e_{t\rho}$, $e_{t\varphi}$, $e_{r\rho}$ and $e_{r\varphi}$ are the corresponding error standard deviations. The discretized direction estimation grid is considered from $-90°$ to $90°$, and its uniform cell size is chosen as $0.05°$. Besides, the signal-to-noise ratio is defined as

$$\mathrm{SNR} = 10\log_{10}(||\mathbf{\Gamma AS}||_F^2/||\mathbf{N}||_F^2) \tag{30}$$

where $\mathbf{S} = [\mathbf{s}(1), \mathbf{s}(2), \ldots, \mathbf{s}(J)]$ and $\mathbf{N} = [\mathbf{n}(1), \mathbf{n}(2), \ldots, \mathbf{n}(J)]$ are signal and noise matrices, respectively.

Fig. 1 (a) and (b) demonstrate the RMSE of DOA estimation versus SNR for Gaussian white noise and colored noise, where $J = 4000$, $e_{t\varphi} = e_{r\varphi} = 20°$, $e_{t\rho} = e_{r\rho} = 0.4$, and there are three uncorrelated targets located at $\theta_1 = -10°$, $\theta_2 = 0°$ and $\theta_3 = 10°$. As can be seen from Fig. 1 (a), RD-MUSIC holds the approximate RMSE with ESPRIT-based algorithm, and adaptive-SR is inferior to the other methods in a wide range of SNR, for in current case, the values of gain-phase errors are too large for adaptive-SR to obtain reliable initial angles. The proposed method performs the best when SNR exceeds about SNR $= -5$ dB, for the reason that the advanced FOC-based design for gain-phase error matrix estimation guarantees the successful implementation of sparse representation manner, and the reweighted matrix in sparse representation framework enhances the sparse solution. In Fig. 1 (b), it is clearly verified that the proposed method provides the best DOA estimation performance, because the application of fourth-order cumulants successfully suppresses colored noises, while they lead to serious performance degradation in the other analyzed methods, especially in low SNR region. Furthermore, when SNR $= -10$ dB, RD-MUSIC is invalid, and adaptive-SR algorithm is unable to be convergent.

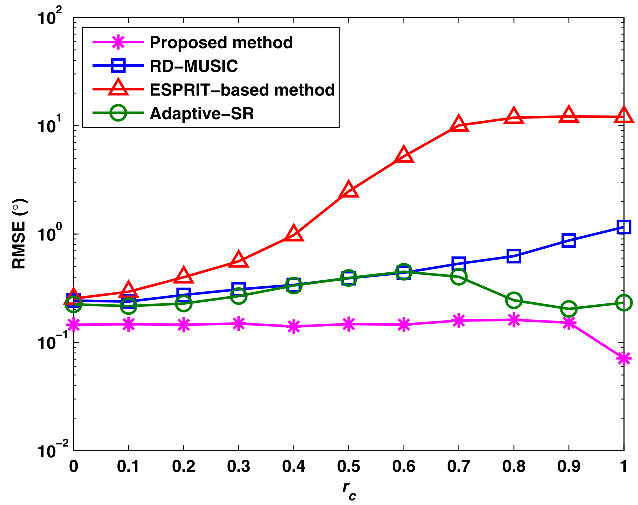

Fig. 2. RMSE versus correlation level of colored noise with three targets and SNR = 0 dB.

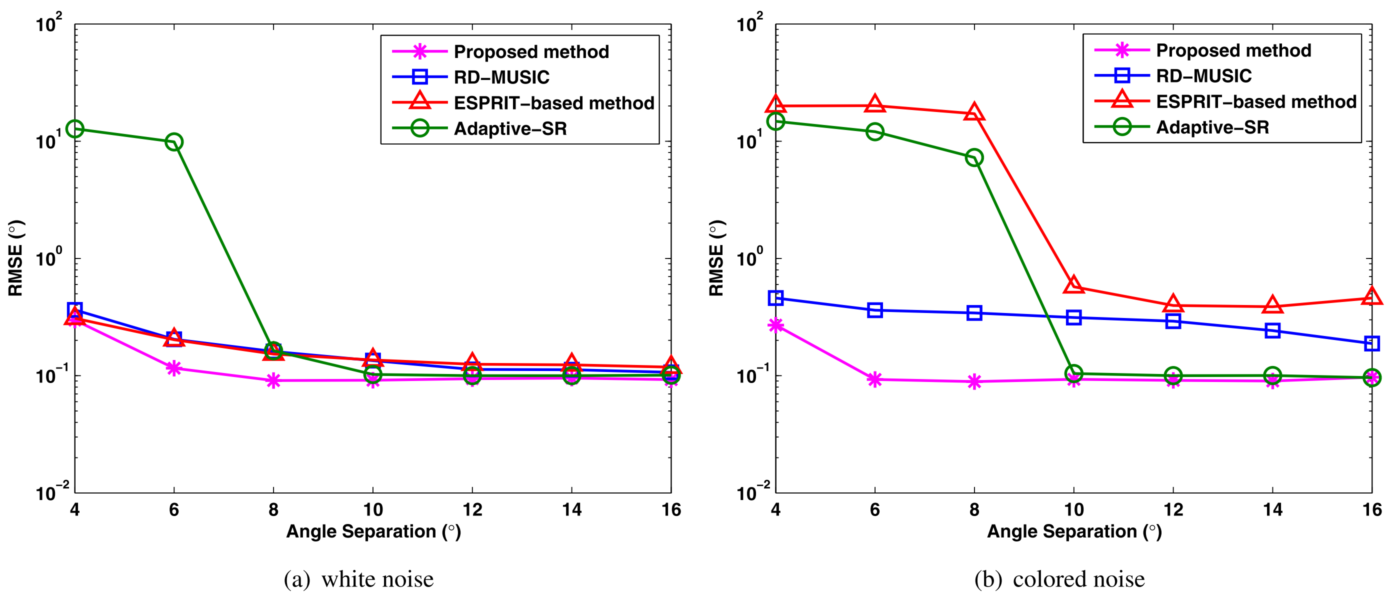

Fig. 3. RMSE versus angle separation with two targets and SNR = 0 dB.

Fig. 2 depicts the RMSE of DOA estimation versus the correlation level of Gaussian colored noise, with SNR = 0 dB, which is commonly used for performance evaluation of DOA estimation [42]. In Fig. 2, $J = 2000$, r_c varies from $r_c = 0$ to $r_c = 1$, and the other conditions are the same with Fig. 1. From Fig. 2, it can be concluded that the proposed method provides superior DOA estimation in all range of r_c, and the performance does not depend on the level of colored noise correlation. Furthermore, the estimation superiorities of the proposed method over ESPRIT-based algorithm and RD-MUSIC are increasingly obvious with the increasing of noise correlation level.

Fig. 3 (a) and (b) illustrate the RMSE versus angle separation for Gaussian white noise and colored noise, respectively, where $J = 4000$, SNR = 0 dB, $e_{t\varphi} = e_{r\varphi} = 10°$ and $e_{t\rho} = e_{r\rho} = 0.3$. Two targets with $\theta_1 = 0°$ and $\theta_2 = 0° + \Delta\theta$ are considered, $\Delta\theta$ varies from 4° to 16°. It can be seen from Fig. 3 (a) that adaptive-SR algorithm is inferior to the others with small $\Delta\theta$, and in Gaussian white noise condition, the four methods have the similar DOA estimation performance when the angle separation exceeds about $\Delta\theta = 10°$. On the other hand, Fig. 3 (b) verifies that with colored noise, the proposed method performs the best and owns the highest spatial angular resolution, by contrast, the performance of ESPRIT-based algorithm and RD-MUSIC is greatly influenced, especially when the angle separation is small.

Fig. 4 (a) and (b) show the RMSE of DOA estimation versus snapshots for Gaussian white noise and colored noise, respectively, where SNR = 5 dB, $e_{t\varphi} = e_{r\varphi} = 10°$, $e_{t\rho} = e_{r\rho} = 0.3$, and the DOAs of three uncorrelated targets are $\theta_1 = -11.5°$, $\theta_2 = 0°$ and $\theta_3 = 11.5°$. It can be observed from Fig. 4 (a) and (b) that adaptive-SR algorithm holds similar RMSE in all snapshot region. Moreover, when the number of the snapshots varies from $J = 700$ to $J = 4900$, the proposed method owns the lowest RMSE. With the increased J, the proposed method stands out clearly from the other methods, no matter whether the Gaussian noise is white or colored.

Fig. 5 (a) and (b) illustrate the target resolution probability of different methods versus SNR for Gaussian white noise and colored noise, respectively, where $J = 2000$, $e_{t\varphi} = e_{r\varphi} = 8°$, $e_{t\rho} = e_{r\rho} = 0.2$, and three uncorrelated targets are located at $\theta_1 = -11.5°$, $\theta_2 = 0°$ and $\theta_3 = 11.5°$. With the estimation results $\hat{\theta}_{1,i}$, $\hat{\theta}_{2,i}$ and $\hat{\theta}_{3,i}$, the ith Monte Carlo trial is considered as a success if the absolute values of the estimation errors satisfy $\max\{|\hat{\theta}_{1,i} - \theta_1|, |\hat{\theta}_{2,i} - \theta_2|, |\hat{\theta}_{3,i} - \theta_3|\} \le 0.1°$. After all the $Q = 500$ trials, let $\hat{Q}_s$ denote the total number of the successful trials. The target resolution probability is defined as $\hat{Q}_s/Q$. It can be concluded from the figures that for both Gaussian

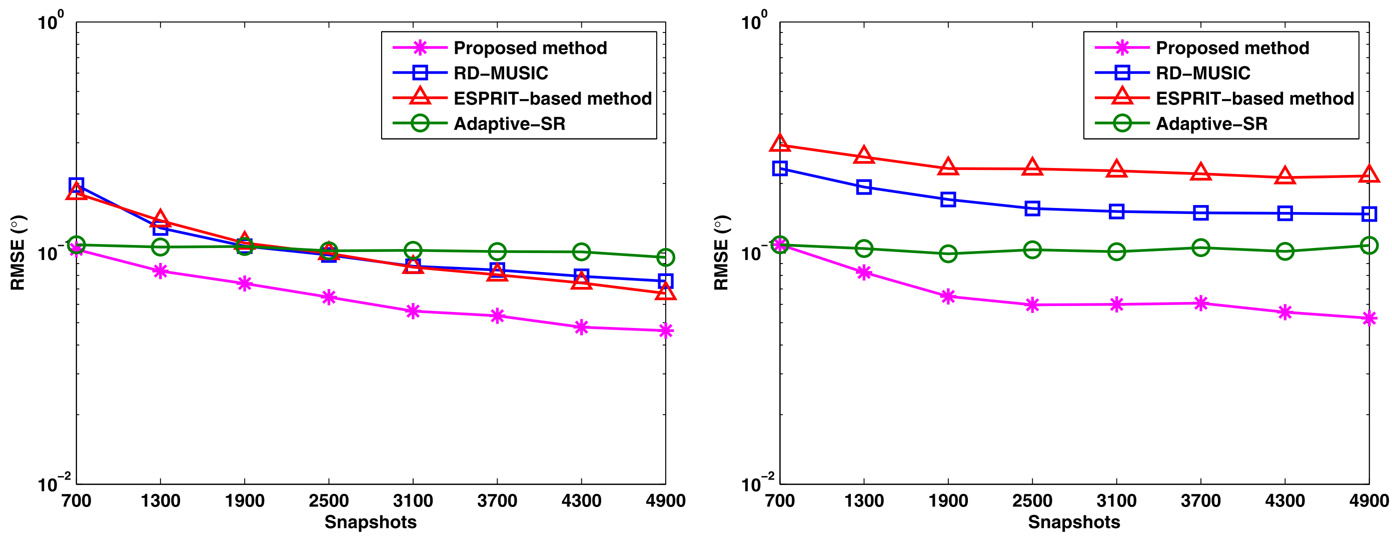

(a) white noise (b) colored noise

Fig. 4. RMSE versus snapshots with three targets and SNR = 5 dB.

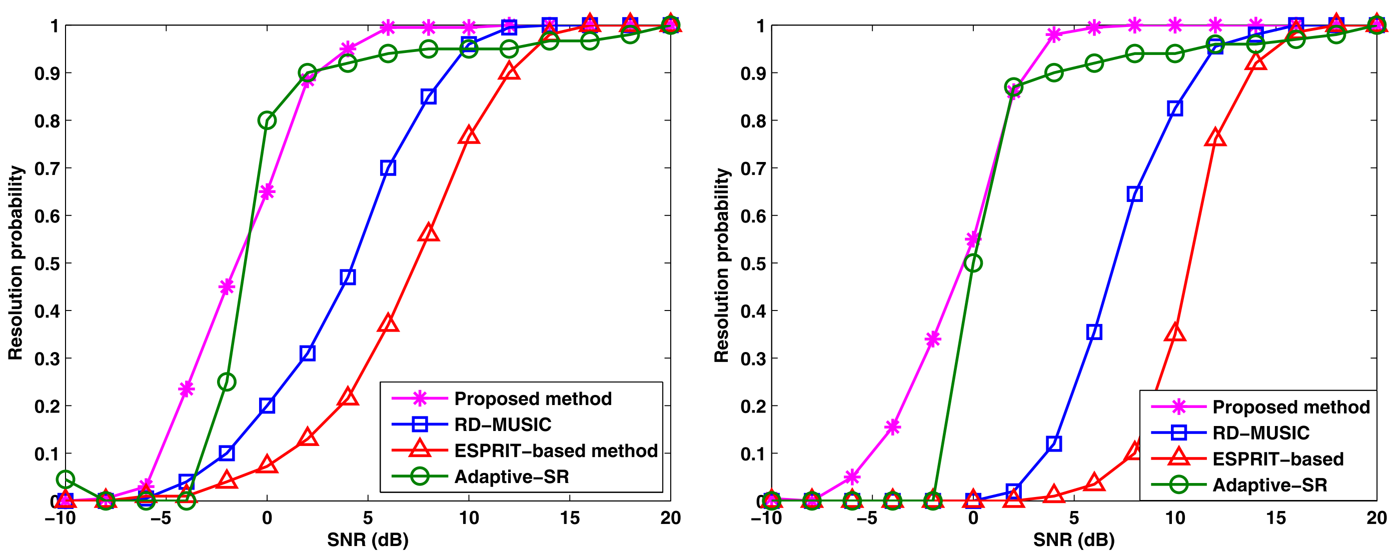

(a) white noise (b) colored noise

Fig. 5. Target resolution probability versus SNR with three targets.

white and Gaussian colored noise conditions, when the SNR is high enough, all methods provide almost 100% target resolution probability, and when the SNR decreases, with prominent superiority over ESPRIT-based method and RD-MUSIC, the proposed method provides better resolution probability.

Fig. 6 (a) and (b) show the RMSE of DOA estimation versus gain-phase errors for Gaussian white noise and colored noise, respectively, $e_\rho = e_{t\rho} = e_{r\rho}$, $e_\phi = e_{t\varphi} = e_{r\varphi}$, (e_ρ, e_ϕ) varies from $(0.1, 4°)$ to $(1, 40°)$, SNR = 0 dB, $J = 4000$, and the angles of three uncorrelated targets are assumed as $\theta_1 = -10°$, $\theta_2 = 0°$ and $\theta_3 = 10°$. The figures indicate that ESPRIT-based algorithm, RD-MUSIC and the proposed method perform independently of the errors, while the performance of adaptive-SR degrades as e_ρ and e_ϕ increase, for its initial angle errors become larger. Additionally, the proposed method is superior to the other algorithms in all error region for both Fig. 6 (a) and (b).

6. Conclusion

In this paper, for monostatic MIMO radar in the presence of gain-phase errors, we have proposed a sparse DOA estimation algorithm with the FOC-based error matrix estimation. The proposed algorithm is applicable for MIMO radar with partly-calibrated uniform linear arrays. By the use of fourth-order cumulants and dimensional reduction, the proposed method firstly obtains a reliable gain-phase error matrix with a low dimension. Then exploiting the estimated error matrix, accurate DOA estimation is achieved by solving the reweighted sparse representation framework. The computational complexity is analyzed, and the simulation results verify that for both white and colored Gaussian noise conditions, the proposed method performs well in a wide range of gain-phase errors, and it provides better angle estimation performance and higher spatial angular resolution than RD-MUSIC, adaptive-SR and ESPRIT-based algorithms.

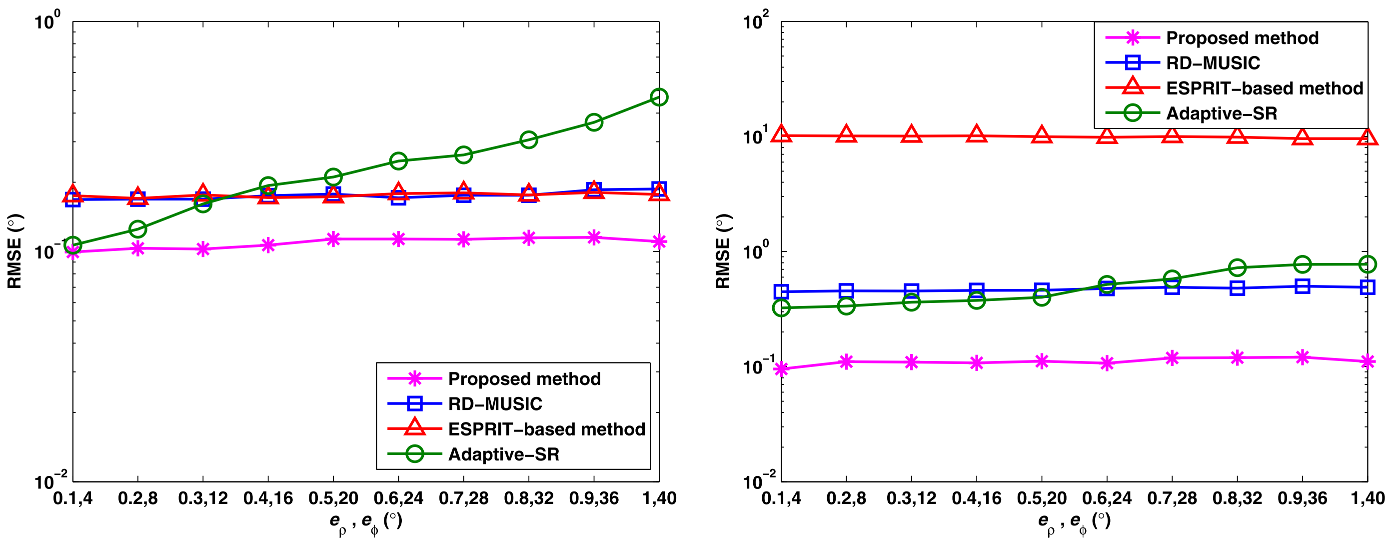

(a) white noise (b) colored noise

Fig. 6. RMSE versus gain-phase errors with three targets and SNR = 0 dB.

Acknowledgments

This work was supported by the China Scholarship Council (CSC, No. 201506680027), and the Fundamental Research Funds for the Central Universities (HEUCF160401).

References

[1] E. Fishler, A. Haimovich, R. Blum, Performance of MIMO radar systems: advantages of angular diversity, in: Proceeding of the Thirty-Eighth Asilomar Conference on Signals, Systems and Computers, 2004, pp. 305–309.
[2] A.M. Haimovich, R.S. Blum, L.J. Cimini, MIMO radar with widely separated antennas, IEEE Signal Process. Mag. 25 (1) (2008) 116–129.
[3] J. Li, P. Stoica, MIMO radar with colocated antennas, IEEE Signal Process. Mag. 24 (5) (2007) 106–114.
[4] A.M. Elbir, T.E. Tuncer, 2-D DOA and mutual coupling coefficient estimation for arbitrary array structures with single and multiple snapshots, Digit. Signal Process. 54 (7) (2016) 75–86.
[5] J.F. Li, X.F. Zhang, Two-dimensional angle estimation for monostatic MIMO arbitrary array with velocity receive sensors and unknown locations, Digit. Signal Process. 24 (1) (2014) 34–41.
[6] X. Gao, X.F. Zhang, et al., On the MUSIC-derived approaches of angle estimation for bistatic MIMO radar, in: Proc. Int'l Conf. Wireless Networks and Inf. Syst., 2009, pp. 343–346.
[7] C. duofang, C. Baixiao, et al., Angle estimation using ESPRIT in MIMO radar, Electron. Lett. 44 (12) (2008) 770–771.
[8] H.D. Yan, J. Li, et al., Multitarget identification and localization using bistatic MIMO radar systems, EURASIP J. Adv. Signal Process. 2008 (2008) 48.
[9] X. Zhang, Y. Huang, et al., Reduced-complexity Capon for direction of arrival estimation in a monostatic multiple-input multiple-output radar, IET Radar Sonar Navig. 8 (8) (2012) 796–801.
[10] G.M. Zheng, B.X. Chen, et al., Unitary ESPRIT algorithm for bistatic MIMO radar, Electron. Lett. 48 (3) (2012) 179–181.
[11] D. Malioutov, M. Cetin, A.S. Willsky, A sparse signal reconstruction perspective for source localization with sensor arrays, IEEE Trans. Signal Process. 53 (8) (2005) 3010–3022.
[12] J. Yin, T. Chen, Direction-of-arrival estimation using a sparse representation of array covariance vectors, IEEE Trans. Signal Process. 59 (9) (2011) 4489–4493.
[13] X. Xu, X. Wei, Z. Ye, DOA estimation based on sparse signal recovery utilizing weighted l_1-norm penalty, IEEE Signal Process. Lett. 19 (3) (2012) 155–158.
[14] Z.Q. He, Z.P. Shi, L. Huang, Covariance sparsity-aware DOA estimation for nonuniform noise, Digit. Signal Process. 28 (5) (2014) 75–81.
[15] X.P. Wang, W. Wang, J. Liu, A sparse representation scheme for angle estimation in monostatic MIMO radar, Signal Process. 104 (11) (2014) 258–263.
[16] K. Sun, Y. Liu, et al., Adaptive sparse representation for source localization with gain/phase errors, Sensors 11 (5) (2011) 4780–4793.
[17] B. Liao, S.C. Chan, Direction finding with partly calibrated uniform linear array, IEEE Trans. Antennas Propag. 60 (2) (2012) 922–929.
[18] T. Li, A. Nehorai, Maximum likelihood direction finding in spatially colored noise fields using sparse sensor arrays, IEEE Trans. Signal Process. 59 (3) (2011) 1048–1062.
[19] X.L. Liu, G.S. Liao, et al., Multitarget localization and estimation of gain-phase error for bistatic MIMO radar, Acta Electron. Sin. 39 (3) (2011) 596–601.
[20] Y.D. Guo, Y.S. Zhang, ESPRIT-like angle estimation for bistatic MIMO radar with gain and phase uncertainties, Electron. Lett. 47 (17) (2011) 996–997.
[21] J. Li, M. Jin, et al., Transmit and receive array gain-phase error estimation in bistatic MIMO radar, IEEE Antennas Wirel. Propag. Lett. 14 (2015) 32–35.
[22] J. Li, X. Zhang, et al., Reduced-dimension MUSIC for angle and array gain-phase error estimation in bistatic MIMO radar, IEEE Commun. Lett. 17 (3) (2013) 443–446.
[23] B. Porat, B. Friedlander, Direction finding algorithms based on high-order statistics, IEEE Trans. Signal Process. 39 (9) (1991) 2016–2024.
[24] Z. Ye, Y. Zhang, DOA estimation for non-Gaussian signals using fourth-order cumulants, IET Microw. Antennas Propag. 3 (7) (2009) 1069–1078.
[25] S. Li, X.X. Jiang, et al., Direction of arrival estimation via sparse representation of fourth order statistics, in: IEEE International Conference on Signal Processing, Communication and Computing (ICSPCC), 2013, pp. 1–4.
[26] J. Liu, W.D. Zhou, X.P. Wang, Fourth-order cumulants-based sparse representation approach for DOA estimation in MIMO radar with unknown mutual coupling, Signal Process. 128 (11) (2016) 123–130.
[27] I. Bekkerman, J. Tabrikian, Target detection and localization using MIMO radars and sonars, IEEE Trans. Signal Process. 54 (10) (2006) 3873–3883.
[28] X. Wang, W. Wang, X. Li, J. Liu, Real-valued covariance vector sparsity-inducing DOA estimation for monostatic MIMO radar, Sensors 15 (11) (2015) 28271–28286.
[29] M.L. Bencheikh, Y. Wang, Non circular ESPRIT-RootMUSIC joint DOA-DOD estimation in bistatic MIMO radar, in: 2011 7th International Workshop on Systems, Signal Processing and their Applications (WOSSPA), Tipaza, Algeria, 9–11 May 2011, pp. 51–54.
[30] B. Liao, S.C. Chan, Direction finding in MIMO radar with unknown transmitter and/or receiver gains and phases, Multidimens. Syst. Signal Process. (2015) 1–17.
[31] G.M. Zheng, J. Tang, X. Yang, ESPRIT and unitary ESPRIT algorithms for coexistence of circular and noncircular signals in bistatic MIMO radar, IEEE Access 4 (2016) 7232–7240.
[32] W.T. Shi, J.G. Huang, et al., Orthogonal waveforms design and performance analysis for MIMO sonar, in: IEEE 10th International Conference on Signal Processing (ICSP), 2010.
[33] B. Liao, S.C. Chan, Direction finding in partly calibrated uniform linear arrays with unknown gains and phases, IEEE Trans. Aerosp. Electron. Syst. 51 (1) (2015) 217–227.

[34] J.F. Li, X.F. Zhang, X. Gao, A Joint scheme for angle and array gain-phase error estimation in bistatic MIMO radar, IEEE Geosci. Remote Sens. Lett. 10 (6) (2013) 1478–1482.
[35] J.F. Sturm, Using SeDuMi, a Matlab toolbox for optimization over symmetric cones, Optim. Methods Softw. 11–12 (2009) 625–653.
[36] M. Grant, S. Boyd, CVX: MATLAB Software for Disciplined Convex Programming, version 1.22 (2012).
[37] M. Wax, T. Kailath, Detection of signals by information theoretic criteria, IEEE Trans. Acoust. Speech Signal Process. 33 (2) (1985) 387–392.
[38] J. Liu, X. Wang, W. Zhou, Covariance vector sparsity-aware DOA estimation for monostatic MIMO radar with unknown mutual coupling, Signal Process. 119 (2) (2016) 21–27.
[39] M.E. Davies, Y.C. Eldar, Rank awareness in joint sparse recovery, IEEE Trans. Inf. Theory 58 (2) (2012) 1135–1146.
[40] J.F. Li, J. Ding, D.F. Jiang, Joint direction finding and array calibration method for MIMO radar with unknown gain phase errors, IET Microw. Antennas Propag. 10 (14) (2016) 1563–1569.
[41] X.P. Wang, W. Wang, et al., Sparsity-aware DOA estimation scheme for noncircular source in MIMO radar, Sensors 16 (4) (2016) 539.
[42] C. Zhang, H.P. Huang, B. Liao, Direction finding in MIMO radar with unknown mutual coupling, IEEE Access 5 (2017) 4439–4447.

Jing Liu was born in 1991. She received the B.S. degree in Detection, Guidance and Control Techniques from Harbin Engineering University (HEU), China, in 2013. Since 2014, she has been pursuing the Ph.D. degree in Control Science and Engineering at Department of Automation, Harbin Engineering University (HEU), China. Since 2015, she has also been a joint Ph.D. student funded by the China Scholarship Council, at School of Electrical, Electronic and Computer Engineering, The University of Western Australia (UWA), Australia. Her main research interests are array signal processing, radar signal processing, signal detection, compressed sensing, and array error calibration.

Weidong Zhou received the B.S. and M.S. degrees in Automatic Control from Harbin Institute of Technology in 1988, and Harbin University of Science and Technology in 1991, respectively. He received the Ph.D. degree in Navigation from Harbin Engineering University (HEU), China, in 2006. Since 2005, he has been a full professor at Department of Automation, Harbin Engineering University (HEU), China. He is a editorial board member of the Chinese Society of Architects and Marine Engineering, a member of National Marine Boat Standardization Technical Committee, and a member of the Northeast Regional Branch of the Chinese Society of Inertial Technology. His research interests include the direction of the automatic control theory, integration navigation, estimation theory, computer control, and multi-sensor data fusion.

Xianpeng Wang was born in 1986. He received his M.S. degree and Ph.D. degree in the College of Automation from Harbin Engineering University (HEU), Harbin, China, in 2012 and 2015, respectively. He was a full-time Postdoctoral Research Fellow in the School of Electrical and Electronic Engineering, Nanyang Technological University, Singapore, from 2015 to 2016. Now, he is a professor in the College of Information Science & Technology at Hainan University. He is the author of over 40 papers published in related journals and international conference proceedings, and has served as a reviewer of over twenty journals. His major research interests include communication system, array signal processing, radar signal processing, compressed sensing and its applications.

Defeng (David) Huang received the B. E. E. E. and M. E. E. E. degree in electronic engineering from Tsinghua University, Beijing, China, in 1996 and 1999, respectively, and the Ph.D. degree in electrical and electronic engineering from the Hong Kong University of Science and Technology (HKUST), Kowloon, Hong Kong, in 2004. He joined the School of Electrical, Electronic and Computer Engineering at the University of Western Australia in 2005 as a lecturer, and has been promoted to be a professor with the same school since 2011. Before joining UWA, he was a lecturer at Tsinghua University. He served as an Editor (2011–2015) for the IEEE Wireless Communications Letters, an Editor (2005–2011) for the IEEE Transactions on Wireless Communications, and the Editorial Assistant (2002–2004) to the IEEE Transactions on Wireless Communications.